METALLACARBORANES FOR PROTON THERAPY USING RESEARCH ACCELERATORS: A PILOT STUDY

Teresa PINHEIRO
IBB, Instituto de Bioengenharia e Biociências, Departamento de Engenharia e Ciências Nucleares, Instituto Superior Técnico, Universidade de Lisboa
Lisboa, Portugal
Email: teresa.pinheiro@tecnico.ulisboa.pt

Luis C. ALVES
Centro de Ciências e Tecnologias Nucleares, Departamento de Engenharia e Ciências Nucleares, Instituto Superior Técnico, Universidade de Lisboa, Lisboa, Portugal

Victoria CORREGIDOR
Centro de Ciências e Tecnologias Nucleares, Departamento de Engenharia e Ciências Nucleares, Instituto Superior Técnico, Universidade de Lisboa
Lisboa, Portugal

Francesc TEIXIDOR
Institut de Ciència de Materials de Barcelona (ICMAB-CSIC), Campus UAB, 08193 Bellaterra Barcelona, Spain.

Clara VIÑAS
Institut de Ciència de Materials de Barcelona (ICMAB-CSIC), Campus UAB, 08193 Bellaterra Barcelona, Spain.

Fernanda MARQUES
Centro de Ciências e Tecnologias Nucleares, Departamento de Engenharia e Ciências Nucleares, Instituto Superior Técnico, Universidade de Lisboa
Lisboa, Portugal

Abstract

The feasibility of using an external beam microprobe facility to explore the biological effects generated by proton irradiation in cultured cells is demonstrated. An in-air irradiation set-up was developed that allows energy tuning and enables estimating the flux and dose deposition in cells. A pilot study on the effect new of metallacarborane molecules as radiosensitizer towards human glioblastoma cells was carried out. This served as a proof of concept for the enhancement effect of proton irradiation induced by the presence of boron in the compounds, which undergoes fusion via the $^{11}B(p,\alpha)\alpha\alpha$ reaction. Details of the experimental set-up and physical parameters measured are presented. Also, preliminary results of cell's irradiation and uncertainties are discussed anticipating the advances that have been achieved by our group in this field.

1. INTRODUCTION

The use of energetic proton beams offers advantages in cancer treatment including tumour confinement and higher LET (linear energy transfer). Recently, new drugs with greater selectivity for tumour cells that enable increasing the RBE (relative biological effectiveness) for protons have been investigated. These new drugs are constituted by carborane boron clusters, containing 10 atoms of boron each, coordinated by a central metal ion [1]. The theoretical background of the use of metallacarboranes as radiosensitizers is the presence of boron, which may increase the effect of protons on cell death due to the $^{11}B(p,\alpha)\alpha\alpha$ nuclear fusion reaction [2]. This reaction shows a major resonance near $E_p = 0.675$ MeV with isotropic distribution and a high cross section of the order of 1 barn. The reaction consists of a two-step sequential decay yielding three α-particles. The de-excitation of ^{12}C, the first intermediate reaction product, yields one α-particle with energy near 4 MeV and ^{8}Be, which in turns splits in two α-particles of 2.74 MeV each [3-5].

Due to these characteristics, the reaction has become very attractive in the context of medical applications of proton therapy as emitted α-particles range in water is of the order of a cell dimension. In this context, energetic

beams generated by research accelerators can be useful to demonstrate the potential of metallacarboranes as radiosensitizers for proton therapy. This is very important for proton therapy modality, as there is an urgent need to improve the efficacy of protons in cancer treatment. Thus, enhancing local dose inside tumours upon exposure to radiation, increasing RBE for protons, and reducing the effective radiation dose are factors that ultimately converge to improve the efficacy of treatment [1,6]. This can be achieved through a synergistic cell-killing effect of metallacarboranes when combined with radiation.

2. STUDY DESIGN

By using research accelerators to generate energetic protons and by extracting the proton beam to air, live cells can be irradiated under controlled conditions, and their dose-dependent viability subsequently assessed. Therefore, a pilot study was planned to demonstrate the enhancement effect of proton-boron reaction in cell-killing. To assess the biological effects, a tumour cell model (human glioblastoma, U87 cells) exposed to new metallacarborane compounds (Fe-carborane, FeC, and an iodinated analog, I_2FeC) was used. The cellular viability as a function of deposited dose will be used as the endpoint for the effect of proton irradiation. Details of the experimental setup, geometry of irradiation, energy tuning of the proton beam, physical parameters measured and calculated as well as cell irradiation protocol will be comprehensively described in the sections below.

3. EXPERIMENTAL SETUP

Experiments were done at ambient pressure using the external beam facility of the nuclear microprobe (Oxford Microbeams Ltd., UK) installed at the 2.5 MV single ended Van de Graaff accelerator of the IST (Instituto Superior Técnico, Universidade de Lisboa, Portugal) [7,8]. The technical details of the nuclear microprobe and external beam facility were previously described [8-10].

In Fig. 1 the schematic of the nuclear microprobe and experimental setup used in this study can be depicted. The beam is extracted from the vacuum chamber to air through an exit nozzle. In the particular set-up used in this study, a nozzle with 2.9 mm internal diameter was used to extract the beam through a 6.3 µm thick Mylar window and scanned over an area of interest. The 96-well plate (where the cells are incubated) was positioned perpendicular to the beam path on a x-y-z table. The distance of the sample (cell monolayer at the bottom of the wells) from the exit window was of 13.4 mm. In this pathway besides the 6.3 µm thick Mylar window of the exit nozzle, a 12.6 µm thick Mylar window covering the 96-well plate was used, separating the air path, which is fractionated in two sections, i.e., 2mm from the exit nozzle to the Mylar cover of the plate and 11.4 mm to the bottom of the well.

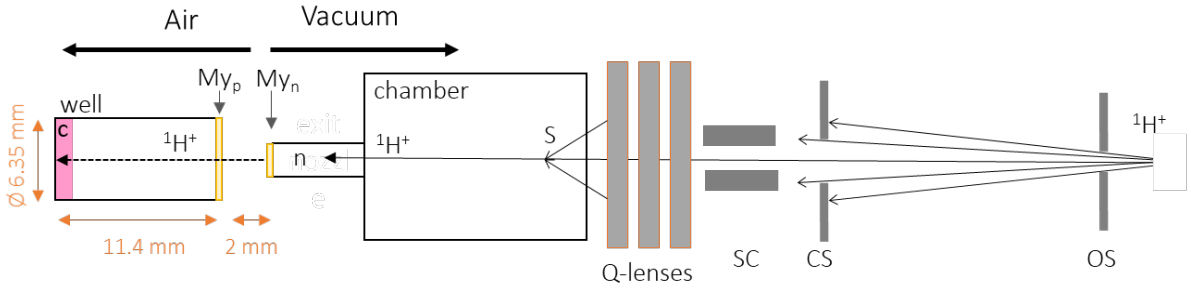

FIG. 1. The IST nuclear microprobe schematic (not on scale) including the external beam setup used for cell irradiation. The microprobe configuration consists of object slits (OS) for beam current control, collimation slits (CS) for beam divergence control, the magnetic quadrupole triplet (Q-lenses) [7] for beam focusing on the focus plane (S) inside the irradiation chamber (vacuum) where the sample is positioned. The scanning coils (SC) are located before the lenses. The vacuum chamber configuration accommodates several detectors [7,8] and enables the adaptation, at the rear, of a cylindrical cap having at its end a nozzle (n) supporting a vacuum tight extraction window (My_n). The schematic of the setup for cell irradiation in air represents one unit well of a typical 96-well plate for cell culture. In the used experimental configuration, the extracted $^1H^+$ beam encountered the cell monolayer (c) after traversing the air path and a Mylar foil (My_p) which covers the cell culture plate. The external set-up includes a x-y-z table for sample positioning, enables detectors for sample characterization (e.g., PIXE) and accommodates a minicamera that helps on sample visualization and alignment [9,10].

3.1. Calculation of the energy loss

The 2.0 MeV proton energy was tuned to ensure that the resonance energy near E_p = 0.675 MeV of the $^{11}B(p,\alpha)\alpha\alpha$ nuclear fusion reaction was reached at the sample cell layer. Both air and Mylar foils served as attenuators for the proton beam. The calculations were carried out using SRIM opensource software [11]. The sequence of attenuators consisted of: 1) Mylar foil of 6.3 µm thickness for extraction the proton beam from vacuum to air; 2) 2 mm air path; 3) Mylar foil of 12.6 µm thickness covering the 96-well plate where cells were incubated; 4) 11.4 mm air path. The beam encountered the cell layer with an entrance energy of 1.27 MeV. The energy loss in the cell layer was also simulated with SRIM, considering liquid water as a medium equivalent to a cell. The transmitted energy in 30 µm and 40 µm water (estimated cell layer thickness; see section 4) and corresponding LET is displayed in Table 1.

TABLE 1. SRIM simulations [11] of transmitted energy in the cell layer for an entrance energy of 1.27 MeV protons (simulation nº of particles =1000; values are x±SD) and the corresponding value of LET.

Cell Layer thickness (µm)	Transmitted energy (keV)	LET (keV/µm)
30	477±28	26.43
40	15±2	31.38

3.2. Beam focusing and scan size estimation

A proton beam of 2.0 MeV was focused (triplet of quadrupole lenses, Oxford Microbeams Ltd. [7]) in vacuum [7] to dimensions of ~3×4 µm^2. When the beam is extracted to air the spatial resolution degrades compared to analysis performed in vacuum, mainly due to beam divergence. For routine conditions (with beam currents of ~100 pA) typical spatial resolution of ~70×70 µm^2 can be achieved [8,10]. The beam resolution quality can be verified using a microscopy copper grid positioned at a convenient distance from the exit nozzle that allows the accommodation of a PIXE detector. Thus, scanning the beam over the sample an image of the grid can be obtained (Fig. 2-A). Most importantly, the grid imaging is an adequate methodology to define the scan dimension and to ensure that the irradiated area is the same for all the samples analysed in the same run. This can be done by setting a mask using the OMDAQ2007 acquisition software features (Fig. 2-B).

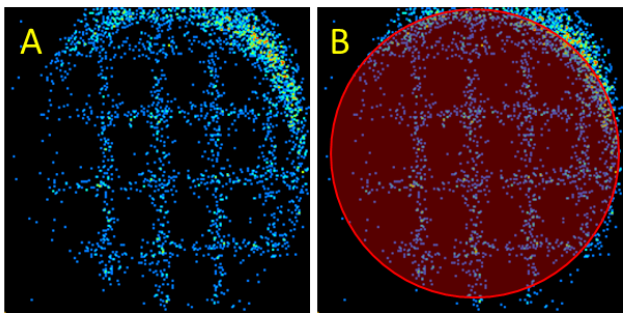

FIG. 2. Image of 50-mesh microscopy copper grid (A) recorded in air at the external microprobe setup and the same image with a mask over-imposed (red circle) delimiting the defined irradiation area (B). Grid specifications: 3.05mm external diameter; pitch 500 µm; hole 450 µm; bar 50 µm).

Although the diameter of the exit nozzle (2.9 mm) sets the limit of the maximum scanning area at the exit, beam divergence across the air path cannot be disregarded. As can be depicted in Fig. 2, the maximum dimensions of the scan at a position of the grid ~3 mm distant from the exit nozzle is larger than the whole area of the microscopy grid (3.05 cm diameter). Thus, to obtain more reliable dimensions of the scan at the position of irradiation on the x-y-z table, a commercial material was used, that emits a bright fluorescence (visible wavelengths) following proton irradiation (Fig. 3). The average size of the irradiated area over 3 runs was 0.134±0.006 cm^2, which represents an uncertainty < 5%. The illuminated area of the target provided the best possible estimation of the irradiation area which is required for further calculation of proton flux and dose.

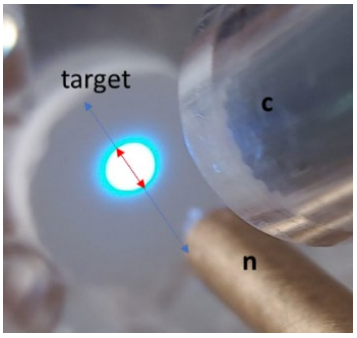

FIG. 3. Photograph of the standard material (target) during proton irradiation showing the bright fluorescence spot that corresponds to the scanned area. The red and blue arrows represent the diameters of the scan (unknown) and the target (known), respectively; n – tip of the nozzle (beam extraction system); c – mini-camera.

In the context of cell irradiation, other relevant parameter to consider is the homogeneous distribution of particles impinging over the sample surface in the defined area. As far as beam stability can be monitored (see section 3.3) the even distribution of protons during irradiation is guaranteed by setting the speed of the scanning (time spent by the beam at each beam position or pixel) at a convenient level (e.g., 10 µs). Therefore, the time required to perform a 256×256 pixels scan is ~ 0.65 s.

3.3. Charge measurement to estimate the flux of protons impinging on the cell layer

In this preliminary study the flux of protons was controlled on real time by monitoring the count rate measured by the acquisition system (OMDAQ2007). During cell irradiation the count rate was kept below 200 Hz, which corresponded to ~1.5-2.5×10^7 protons/s. To estimate the flux of protons impinging on the cell monolayer, the EBS (elastic backscattered spectrometry) spectra of a gold reference material was periodically analyzed to obtain a normalization factor, Q_f [12], to the live charge (Q_{live}), recorded in the acquisition system (OMDAQ2007). The spectra of the gold standard were collected in the vacuum chamber.

The flux can be estimated as in eq. 1:

$$Flux(nº\ of\ protons.cm^2.s^{-1}) = \frac{Q_{live} \times Q_f}{irradiation\ area} \quad \text{Eq. 1.}$$

As reference, a spherical cell of 30 µm diameter irradiated with a flux of 2×10^8 protons.cm^{-2}.s^{-1} receives ca. 1600 protons/s.

To obtain the flux of protons arriving at the cell layers of each irradiated well, an average value of the charge measurements carried out during the entire irradiation run for each assay (before starting the irradiation of the wells, 3-wells intercalary measurements and after irradiation) was considered. Uncertainties in flux calculation were in a range of 20% to 40%, mainly due to fluctuations in beam current and consequently on charge measurements.

4. IRRADIATION OF CELL CULTURES

Glioblastoma U87 cells were grown in 96-well cell plates in an adequate number to form a monolayer. Two Fe carborane compounds, FeC and an iodinated analogue I_2FeC, were used in this study [1]. Cells were incubated for 24h with FeC and I_2FeC. Non-treated cells served as controls. The concentrations of the compounds were selected according to the cytotoxic activity study previously performed. The medium concentrations of FeC and I_2FeC used in this pilot study were 50 µM and 10 µM, respectively, which correspond to concentrations below the IC_{50} value.

After the incubation period the culture medium was replaced with fresh medium before irradiation to ensure that only viable cells remain attached to the bottom of the well and that the FeC and I_2FeC compounds taken up by the cells would be responsible for the observed effects. For each assay two sets of controls (non-treated cells) and cells treated with FeC and I_2FeC compounds were prepared, one was irradiated and another was non-irradiated. Twelve wells (one column of the 96-well plate) were considered in each assay for each condition tested, treated and controls, non-irradiated and irradiated (Fig. 5).

Just before proton irradiation, the excess culture medium was removed, ensuring that just the cell monolayer remains adherent at the bottom of the well with culture medium filling interstitial spaces between cells.

The U87 cell's dimensions are in the range of 20-30 µm. This way, a water equivalent depth of approximately 30-40 µm can be assumed for the cell layer and cells remain with minimal life supporting conditions until the end of the experiment.

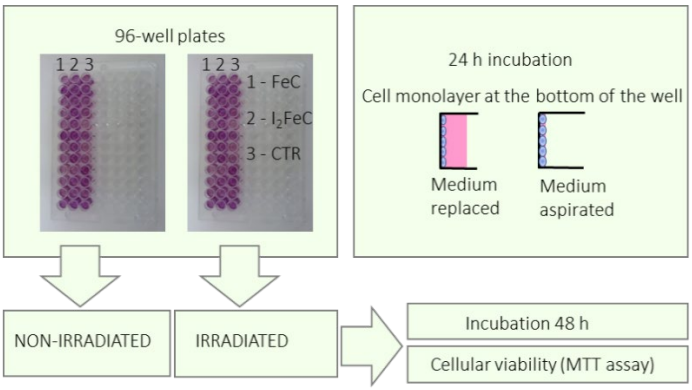

FIG. 5. Schematic of the proton irradiation assay.

The U87 cells were irradiated for 10 s at ambient pressure with a 1.27 MeV proton beam at the entrance of the cell layer, as described above, to ensure that boron resonance of 675 keV was reached within the cell layer. The effective dimensions of the scanned area over the cell layer was ~33% of the total area of the well. The estimated average dose delivered in each well was of 0.98 kGy/s to 1.17 kGy/s, whether considering a 30 or 40 cell layer thickness. In average it can be assumed that a dose of 1 kGy/s was delivered in each well.

The cellular viability as a function of deposited dose was used as the endpoint for the effect of proton irradiation. To this end, after U87 cell's irradiation, fresh medium was added, and cellular viability assessed after 48 h of incubation [13]. A decrease of the cellular viability after proton irradiation was observed for U87 cells. In controls, proton irradiation caused a decrease of approximately 20% relative to non-irradiated cells, whereas in FeC and I_2FeC treated cells a significant decrease of ca. 50% was observed (Fig. 6).

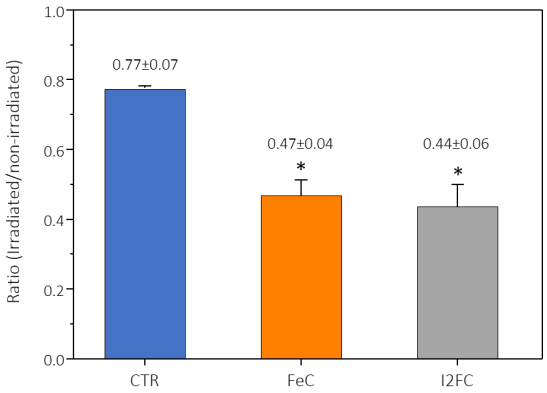

FIG. 6. Viability of U87 cells after proton irradiation, measured with a colorimetric method, the MTT assay. Ratios between irradiated and non-irradiated cells for controls and for those cells treated with FeC and I_2FeC compounds are plotted. Significant differences to non-irradiated cells (*) are indicated in the graph ($p<0.05$).

Noteworthy, only 33% of the cells in each well were irradiated and the viability assay reflects all the cells in the nonolayer (in each well). Nevertheless, a pronounced decrease in the viability of FeC and I_2FeC treated cells after proton irradiation was observed. The effect cannot be attributed to cytotoxicity of Fe carborane compounds against U87 cells. A screening of cytotoxic activity conducted before irradiation showed that for the concentrations used in this study only a small decrease in viability (5-15%) was observed in treated cells when compared to controls. All together the results suggest that a strong cell-killing effect is caused by the presence of Fe carborane compounds in cells following proton irradiation. Recent studies reported on the usefulness of other boron cluster's carriers as radiosensitizers for proton therapy using breast cancer [14] and prostate cancer [15] cell lines.

5. FINAL REMARKS

The magnitude of the decline in the viability of cells incubated with the boron compounds FeC and its iodinated analogue I_2FeC, was well above the direct effects caused by proton irradiation alone in non-treated cells.

The viability decrease observed in our study may derive from α-particles generated in the nuclear fusion reaction as these particles may have direct consequences in the irradiated cells where they are generated and possibly in those contiguous to the irradiated area. The estimated range of these α-particles in water is of the order of 16-25 μm, which is in the range of U87 cell dimensions.

A major limitation of this work refers to the uncertainties in charge determination and therefore on the estimation of dose. Improvements in the experimental setup are ongoing to collect charge during irradiation period of each well. In addition, a validation step with a Monte Carlo (MC) model will be performed to compare several MC and experimental parameters, such as divergence of the beam, energy spectrum, the variation of the Bragg peak depending on the point of reaction and the variation of the maximum dose.

Finally, this pilot study provided evidences for the proof of concept that Fe carboranes, FeC and I_2FeC compounds magnify cell-killing after proton irradiation, acting as radiosensitizers and that the mechanism may be associated with the presence of boron and the nuclear fusion reaction with protons.

ACKNOWLEDGEMENTS

This work was supported by Fundação para a Ciência e Tecnologia (projects UID/Multi/04349/2019, PTDC/MEDQUI/29649/2017, UIDB/04565/2020, UIDP/04565/2020 - iBB/IST and LA/P/0140/2020 - Associate Laboratory Institute for Health and Bioeconomy - i4HB) and from the Spanish Ministerio de Economía y Competitividad (PID2019-106832RB-I00), the Generalitat de Catalunya (2017SGR1720).

REFERENCES

[1] García-Mendiola, T., Bayon-Pizarro, V,. Zaulet, A., Fuentes, I., Pariente, F., Teixidor, F., Viñas, C. Lorenzo, E., Metallacarboranes as tunable redox potential electrochemical indicators for screening of gene mutation. Chem. Sci., 2016, 7, 5786-5797.

[2] Yoon, D.-K., Jung, J.-Y., Suha, T.S., Application of proton boron fusion reaction to radiation therapy: A Monte Carlo simulation study. Appl. Phys Lett 105 (2014) 223507.

[3] Moreau D.C., Potentiality of the proton-boron fuel for controlled thermonuclear fusion. Nucl. Fusion, 17 (1977) 13-20

[4] Spraker, M.C., Ahmed, M.W., Blackston, M.A., Brown, N., France III, R. H., Henshaw, S. S., Perdue, B. A., Prior, R. M., Seo, P.-N., Stave, S, Weller, H.R., The $^{11}B(p,\alpha)^{8}Be \rightarrow \alpha + \alpha$ and the $^{11}B(\alpha,\alpha)^{11}B$ reactions at energies below 5.4 MeV. J. Fusion Energ., 31 (2012) 357–367.

[5] Ruggiero, A.G., Nuclear Fusion of Protons with Boron. Contribution to Conference on Prospects for Heavy Ion Inertial Fusion, Aghia Pelaghia, Crete, Greece, September 26 – October 1 (1992). https://inis.iaea.org/collection/NCLCollectionStore/_Public/24/028/24028563.pdf (accessed 9-6-2022).

[6] Cirrone, G.A.P., Manti, L., Margarone, D., Petringa, G., Giuffrida, L., Minopoli, A., Picciotto, A., Russo, G., Cammarata, F., Pisciotta, P., Perozziello, F.M., Romano, F., Marchese, V., Milluzzo, G., Scuderi, V., Cuttone, G., Korn, G., First experimental proof of Proton Boron Capture Therapy (PBCT) to enhance protontherapy effectiveness. Sci. Rep., 8 (2018) 1141.

[7] http://www.microbeams.co.uk/ (accessed 9-6-2022).

[8] Alves, L.C., Breese, M.B.H., Alves, E., Paúl, A., da Silva, M.R., da Silva M.F., Soares, J.C., Micron-scale analysis of SiC/SiCf composites using the new Lisbon nuclear microprobe. Nucl. Instrum. Meth. B, 161-163 (2000) 334-338.

[9] Corregidor, V., Alves, L.C., Vilarigues, M., Silva, R.C., The external ion beam facility in Portugal for studying culture heritage. e-Conservation Magazine, 22 (2011) 41-52.

[10] Corregidor, V., Oliveira, A.R., Rodrigues, P.A., Alves, L.C., Paintings on copper by the Flemish artist Frans Francken II: PIXE characterization by external beam. Nucl. Instrum. Meth. B, 348 (2015) 291-295.

[11] http://www.srim.org (accessed 9-6-2022).

[12] Grime, G.W., The "Q factor" method: quantitative microPIXE analysis using RBS normalisation. Nucl. Instrum. Meth. B, 109/110 (1996) 170-174.

[13] Marques, A., Belchior, A., Silva, F., Marques, F., Campello, M.P.C., Pinheiro, T., Santos, P., Santos, L., Matos, A.P.A., Paulo, A., Dose Rate Effects on the Selective Radiosensitization of Prostate Cells by GRPR-Targeted Gold Nanoparticles. Int. J. Mol. Sci. 2022, 23, 5279.

[14] Murphy, N., McCarthy, E., Dwyer, R., Farràs, P., Boron clusters as breast cancer therapeutics. J. Inorg. Biochem., 218 (2021) 111412.

[15] Bláha, P., Feoli, C., Agosteo, S., Calvaruso, M., Cammarata, F.P., Catalano, R., Ciocca, M., Cirrone, G.A.P., Conte, V., Cuttone, G., Facoetti, A., Forte, G.I., Giuffrida, L., Magro, G., Margarone, D., Minafra, L., Petringa, G., Pucci, G., Ricciardi, V., Rosa, E., Russo, G., Manti, L., The Proton-Boron Reaction Increases the Radiobiological Effectiveness of Clinical Low- and High-Energy Proton Beams: Novel Experimental Evidence and Perspectives. Front. Oncol., 11 (2021) 682647.